WILEY-VCH

Supporting Information

Strong Second-Harmonic Generation from Au-Al Heterodimers

Jiyong Wang, Jérémy Butet, Gabriel David Bernasconi, Anne-Laure Baudrion, Gaëtan Lévêque, Andreas Horrer, Anke Horneber, Olivier J. F. Martin, Alfred J. Meixner, Monika Fleischer, Pierre-Michel Adam and Dai Zhang**

1. Nanostructure fabrication

After cleaning by acetone and isopropanol in an ultrasonic bath, the substrate (150 μm thick glass cover slip) was coated with a layer of electron-sensitive resist (Poly-Methyl-Metacrylate (PMMA) 950K diluted in Methyl-Iso-Butyl-Ketone (MIBK) at 30g/L in a spin-coater (spinning speed: 3000 rpm, acceleration speed: 4000 rpm/s, duration: 30 s)). The thickness of the resist is expected to be 160 nm, according to the empirical curve of the spinning speed versus the film thickness. After soft baking (convection oven at 170 °C for 3 hours), we spin-coated a thin layer of conductive polymer (Espacer 300Z from Showa Denko Europe) to prevent charge accumulation during the exposure. Then the resist was exposed with the pre-designed patterns by the electron beam of an eLine system (Raith GmbH, Germany). Micrometric cross-markers have been exposed during the same process to allow the precise alignment of the second step lithography. After the conductive polymer was removed in water, the written patterns were developed via a solution of MIBK (diluted with isopropanol). In the development, the exposed areas of the resist were removed. Then a physical vapor deposition (PVD) process was used to coat the sample with a 3 nm thick TiO_2 layer (for adhesion purposes) and a 50 nm thick Au layer. The sample was finally immersed in acetone for more than 3 hours to liftoff the remainder of the resist.The same process was repeated to prepare the sample for the second step lithography. The first automatized and second manual alignment process allows a precision of about 5 nm in the Al nanocylinder placement. It is worth to note that no adhesion layer has been added between the glass substrate and the Al material.

2. Dark-field scattering spectroscopy

Dark-field scattering spectroscopy was used to measure the linear optical properties of the plasmonic nanostructures for comparison. The sample, placed on an inverted microscope (Nikon Ti-U), was illuminated from the air side by a halogen lamp through a dark-field condenser (NA 0.8-0.95). The scattered light coming from the nanostructures was collected from the glass side by a 20x objective with a numerical aperture (NA) of 0.5 and sent to a spectrometer (Ocean Optics QE 65000) through a pin-hole (200 μm diameter). The measured intensity curves were background corrected (using intensity curves measured in an unstructured area of the sample) and normalized by dividing by the (dark-current corrected) lamp spectrum.

3. Nonlinear optical setups

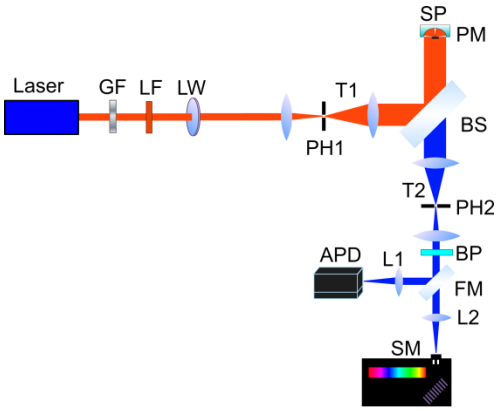

Figure S1. Sketch of the nonlinear optical setup based on a parabolic mirror. GF: gradient filter; LF: Laser line filter; LW: lambda-half wave-plate; T1, 2: telescopes; PH1,2 : pinhole; BS: beam splitter; PM: parabolic mirror; SP: Sample; BP: Band-pass filter; L1,2: Lens; FM: flipping mirror; APD: avalanche photo-diode; SM: spectrometer. For the nonlinear measurements, the incident light is supplied by a femtosecond pulse laser (~110 fs, 89 MHz) with a wavelength centered at 774 nm. The transmission rate can be tuned from 0 to 100% by a gradient neutral density filter.

Figure S1 shows the optical path of the confocal optical microscope. A femtosecond laser (TOPTICA PHOTONICS) generates ultra-short pulses (~110 fs, 89 MHz, 774 nm) in a TEM00 Gaussian mode and was employed to excite the sample. The incident beam passed through a gradient grey filter and a lambda-half wave plate, being able to tune the incident power and excitation polarization, respectively. Afterwards the beam was expanded by a telescope. By using a pinhole within the telescope, undesired and scattered light was filtered out to obtain a homogeneous Gaussian mode. The linearly polarized light was reflected by a non-polarizing dichroic beam splitter towards the parabolic mirror. The parabolic mirror serves both as the focusing element and the emission collector. In air its NA reaches 0.998.[1] Such a high-NA and low-chromatic-aberration mirror enables a high resolution down to the diffraction limit. The emitted optical signal of the nanoparticles was collected and sent through the beam splitter. The dichroic beam splitter excludes the light at the fundamental and higher wavelengths and only transmits the nonlinear information. After reducing the beam size with a second telescope, scattered light is excluded by a pin-hole, and the detection wavelength range was selected by a band-pass filter (370 nm - 680 nm). With a flipping mirror, the beam was either directed towards the spectrometer (Princeton Instruments) to obtain spectral information or to an APD (Single Photon Counting Module - COUNT® BLUE) for point-by-point imaging.

4. Polarization dependent SHG from Au160-Al160 heterodimers

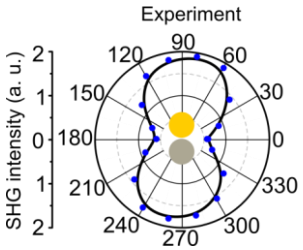

Figure S2. Polarization dependent SHG intensities for the Au160-Al160 heterodimers

Figure S2 shows the experimental (blue dots) results of polarization dependent SHG intensities for the Au160-Al160 heterodimers. The polar angle 0 represents the polarization is along the short axis of nano dimers.

5. Power dependence measurement

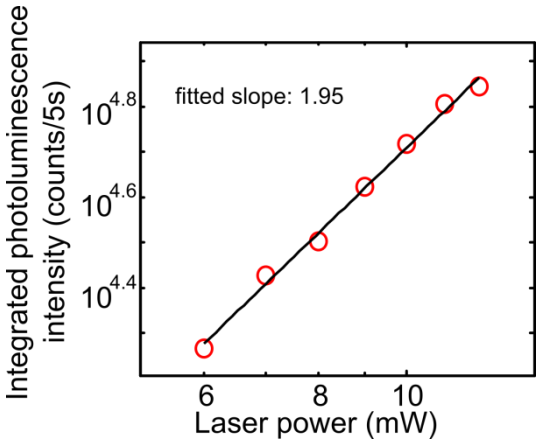

Figure S3. Double logarithmic plot of the emission intensity (spectrally integrated from 390 nm to 650 nm) versus the incident power for aAu160-Al160-G20 heterodimer. The slope value of about 2 indicates a two-photon absorption process. The incident power is measured in front of the parabolic mirror. The excitation polarization is along the long dimer axis.

6. Linear and nonlinear simulations

To disclose the physical origin of second harmonic generation (SHG) responses and explain the results of the experiments, numerical simulations were performed with an in-house surface integral equation (SIE) code giving accurate results for both the near- and the far-field distributions, even in resonant conditions. Dispersive gold dielectric functions are extrapolated from experimental data.[2] The nanostructures are considered to be embedded in an inhomogeneous medium to take into account the influence of the refractive index of the substrate on the surface plasmon resonances. The incident field is always described by a plane wave propagating along the *z*-axis, which is perpendicular to the substrate plan. The linear response is characterized by the backscattering evaluated 50 μm away from the plasmonic nanostructure. As the first step, the linear scattering spectra and the charge distributions are simulated using the SIE method to obtain the information of the local near-field strength. This information is then used for the computation of the SHG intensities.

SIE methods only require the discretization of the surfaces of the metal nanoparticles, exactly where the SHG sources are located, and are therefore extremely well suited for an accurate surface SHG computation.Here we consider only the component of the surface tensor $\chi_{surf,\perp\perp\perp}$, where $\perp$ denotes the component normal to the surface, which is known to dominate the surface response for metallic nanoparticles. In the present case, the nonlinear polarization can be written as $P_{surf,\perp}(\mathbf{r},2\omega)=\chi_{surf,\perp\perp\perp}E_n(\mathbf{r},\omega)\,E_n(\mathbf{r},\omega)$. The SH surface currents are obtained solving the SIE formulation taking into account the nonlinear polarization and enforcing the boundary conditions at the nanostructure surfaces. As the linear surface currents, the SH surface currents are expanded on Rao-Wilton-Glisson basis functions. The expansion coefficients are found applying the method of moments with Galerkin testing. A Poggio-Miller-Chang-Harrington-Wu formulation is used to ensure accurate solutions even at resonant conditions.[3]The SH electric field is then deduced from the SH surface currents using a two-term subtraction method for the evaluation of the Green functions.[4,5] To compare the numerical results with the experimental observations, the SH intensity is integrated over a hemisphere reproducing the light collection performed by the parabolic mirror.

7. Direct comparison between the experiment and the simulation for nanoantennas

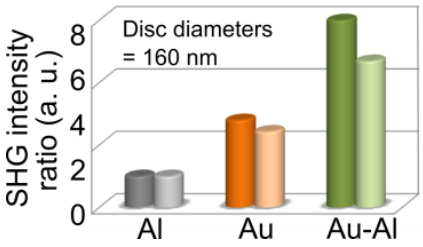

Figure S4. Direct comparison of SHG intensity between the experimental results (left columns, represented by dark colors) and calculated results (right columns, represented by light colors) by using surface integration equations method for the monomers and the heterodimers. The SHG intensities are normalized to the corresponding values of Al NP.

References

[1] M. Lieb, A. Meixner, *Opt.Express* **2001**, 8, 458.
[2] P. B. Johnson, R.-W. Christy, *Phys. Rev. B* **1972**, 6, 12.
[3] A. M.Kern, O. J. F. Martin,*J. Opt. Soc. Am. A***2009**, 26, 732.
[4] P.Ghenuche, S.Cherukulappurath, T. H.Taminiau, N. F. Van Hulst, R. Quidant, *Phys. Rev. Lett.***2008**, 101, 116805.
[5] L.-J. Black, P. R.Wiecha, Y.Wang, C. de Groot, V.Paillard, C. Girard, O. L.Muskens, A. Arbouet, *ACS Photonics* **2015**, 2, 1592.